Post-Access Test Report

Biofouling Analysis for Wave Energy Piston Design

Awardee: Triton Systems, Inc.

Awardee point of contact: Tyler Robertson

Facility: Pacific Northwest National Laboratory – Marine and Coastal Research Laboratory

Facility point of contact: Rob Cavagnaro

Date: 12/13/21

1 INTRODUCTION TO THE PROJECT

Our technical approach is to develop a point-absorber type of WEC to provide power for an ocean observing buoy. WEC is integrated into a separate buoy that is tethered to the ocean observing buoy by a compliant member that transmits power and data but does not influence buoy motion or interfere with measurements. The WEC power buoy takes advantage of the heaving motion of waves to create an oscillating water column to drive a mechanical piston linked to an electrical generator. (See Figure 1).

Figure 1: Triton Power Buoy tethered to ocean buoy

The oscillating water column (OWC) is created by a tube that extends from the WEC buoy to a depth where the effects of surface waves have been largely attenuated. This is referred to as the "wave base" and is typically a depth greater than ¼ of the wavelength of incident waves for waves in "deep water" (defined as where the ocean depth exceeds ½ of the wavelength). Pressure below the wave base is nearly equal to the constant hydrostatic pressure of still-water at that depth and is not significantly influenced by the passing wave trough or crest.

As the WEC buoy-tube body is acted upon by passing waves the lower open end of the tube experiences an oscillating pressure. The upper end of the tube is open to the atmosphere at constant pressure, so the water column experiences an oscillating pressure differential that causes the water column to rise and fall within the tube. (This principle is used to create the sound in whistle buoys.) A piston located at the water free surface in the tube can be connected to a power take off (PTO) to extract energy from the OWC motion. The piston at the water free surface in the tube will oscillate through an elevation change equal to the wave height. The piston reacts against a linear to rotary converter that drives a rotary generator. The generator provides a reacting force that is proportional to the piston velocity. The proportional factor is referred to as the generator damping coefficient, which is related to the load on the generator.

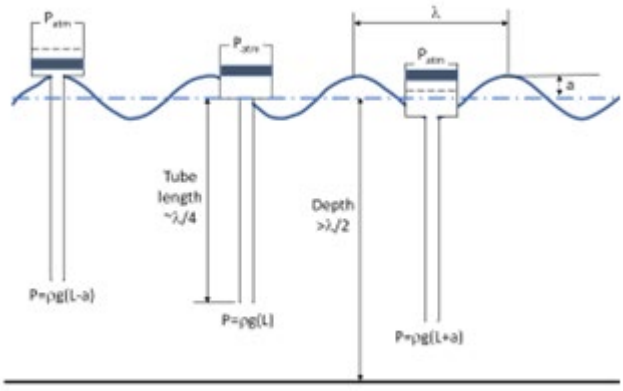

Figure 2: Oscillating Water Column Buoy Motion

The concept of a standalone WEC, was developed based on user feedback. This add-on system would be installed in tandem with an existing ocean buoy to provide power without making major design modifications to the main buoy. This configuration was explored due to the prevalence of scientific measurements happening directly beneath ocean buoys. An integrated wave energy converter would disturb these sensors. An integrated WEC would also most likely require major

design modifications to the main buoy, leading to a reduced chance of adoption. The Triton team evaluated and simulated the concept and determined that the WEC buoy would not negatively impact the motion of the main buoy and would maintain scientific measurement fidelity. (See Figure 3).

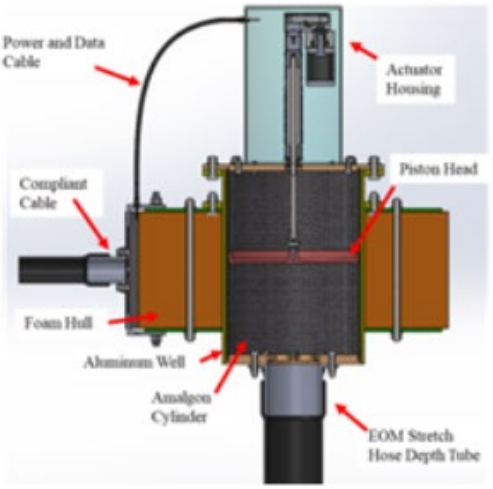

Figure 3: Triton WEC

Technical Assistance Objectives

Triton would like to test the performance of the seal and component materials within the Power Take Off (PTO) assembly, specifically with regards to biofouling. Biofouling has been identified as the biggest risk to the performance of our Wave Energy Converter. Biofouling is also one of the most difficult aspects to test, as it often requires a prolonged deployment in situ, which is expensive and time consuming.

Support being requested through TEAMER

Triton is requesting technical support for the testing of a half-scale PTO prototype to study the effects of biofouling. This testing will take place within controlled biofouling tanks at PNNL, which removes the excessive costs and complexity of open water tests for biofouling.

The study will focus on periodic evaluation of the piston assembly to characterize the growth of biofouling. This evaluation can be done through visual inspection and other quantitative methods, such as weighing of the assembly to calculate added biofouling weight. Caliper measurements can also be taken of the inside surface. In depth biofouling analysis can be performed on material coupons periodically. At the end of the test period, the prototype can be deconstructed and all parts analyzed. An integrated load cell can monitor the resistance experienced by the piston. The current of the actuator can also be monitored as a secondary measurement of resistance or friction.

Two prototype test articles will be compared, one with a biofouling mitigation seal, and one without. The wear and tear on the main dynamic seal will also compared.

This support from PNNL helps meet the Technical Assistance Objectives by providing a controlled environment for evaluating biofouling, which will inform future design improvements and iterations.

2 Roles and Responsibilities of Project Participants

2.1 Applicant Responsibilities and Tasks To Be Performed

Triton Systems

- Provide test articles
- Develop test plan
- Setup/breakdown
- Troubleshooting
- Evaluate results

2.2 Network Facility Responsibilities and Tasks To Be Performed

PNNL

- Develop test plan
- Conduct testing
- Setup/breakdown
- Preprocess data
- Evaluate results

3 Project Objectives

Triton has developed the concept of a biofouling mitigation seal as part of the piston sealing assembly. This mitigation seal has the purpose of preventing the formation of a biofilm on the inside of the piston cylinder. It is hypothesized that the prevention of a biofilm will reduce the amount of macro-biofouling that can occur in the piston assembly. The mitigation seal can also reduce the wear on the main dynamic seal, helping to maintain smooth operation and water-tightness. The cylinder is made from a thermoset composite epoxy, which is resistant to corrosion. However, no studies have researched the material's performance with biofouling. The intake depth tube has also been identified as at-risk for biofouling. Triton would like to evaluate the effect of an oscillating flow on formation of biofouling within the depth tube.

Triton envisions placing one or two prototype PTO assemblies in a PNNL biofouling tank, one with a biofouling mitigation seal and one without, allowing for an evaluation of seal effectiveness at the prevention of biofouling. Samples or coupons of the composite epoxy cylinder material will also be placed in the tank for evaluation of material performance vs biofouling. While there is a focus on specific aspects of the system, this prolonged testing can also be used to evaluate the system as a whole, including seal wear over time, friction, composite epoxy cylinder water absorption, piston corrosion, piston centering, and manufacturing tolerances.

In actual WEC operation, wave action would react against the piston, which would drive the linear actuator and electric generator, providing electrical power. In the test setup, this would be reversed; the linear actuator would be powered to drive the piston in a consistent motion within the cylinder.

This effort is a risk mitigation activity, focused on addressing biofouling before proceeding with open water tests that could fail prematurely due to biofouling and corrosion.

Specific attributes to target:

Seal performance

- Triton is looking for the seal to be performing adequately after the full test period. This includes no visible damage and watertightness above the piston seal.

Reduced biofouling

- Quantifiable reduction in biofouling between control (no mitigation seal) and test article (biofouling mitigation seal)

Material performance

- Materials, including composite cylinder, aluminum baseplate, stainless steel hardware, and seals, withstand seawater corrosion for full test period.

4 Test Facility, Equipment, Software, and Technical Expertise

PNNL Wet Lab Facility

Testing will occur in the PNNL Marine and Coastal Research Laboratory (MCRL) wet laboratory space. The devices under test will be mounted to and operated in a seawater flowthrough tank (Figure 4) 1.5 m in diameter and 0.91 m deep. Unfiltered seawater from Sequim Bay is pumped into and drained from the tank at a fixed rate to ensure circulation. Growth of marine organisms is uncontrolled and entirely dependent on the natural biota within the water, which varies with season and other exogenous conditions in the bay.

PNNL Load Test Equipment

PNNL will provide testing apparatus to measure piston force of the devices under test. Tension and compression of the pistons will be measured with Omega LC203-200 hermetically sealed 200 lbf capacity load cells (Figure 4) excited and amplified with Omega DMD4059 load cell amplifiers. Amplified load measurements will be acquired by a Measurement Computing USB-1608G (or similar) USB data acquisition unit and logged on a computer. Data will be saved as raw .csv files, archived using Microsoft OneDrive, and analyzed using Matlab.

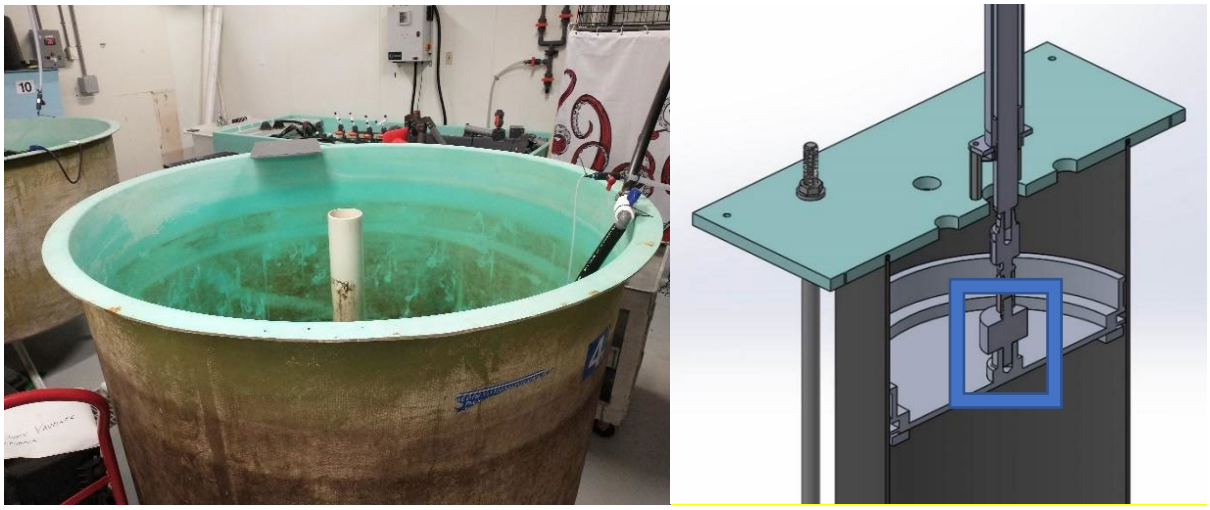

Figure 4: MCRL Wet Lab flow-through tank; Right: Device under test with load cell framed in blue

PNNL Biofouling Analysis Equipment and Facilities

Biofouling analysis tools include high resolution cameras, precision balances, microscopes, and biology equipment/reagents required to stain and visualize biofouling.

PNNL Personnel Expertise

PNNL-MCRL staff expertise encompasses the fields of biology, chemistry and engineering; with specialization in biofouling and corrosion, electrical and mechanical engineering, microscopy, and applied marine technology.

Figure 5: PNNL-MCRL active biofouling experiment

5 Test or Analysis Article Description

Device Under Test

The device under test is a half scale Power Take Off based on Triton's conceptual design. It will consist of a linear actuator, piston head, composite epoxy cylinder, and biofouling mitigation seals. (Figure 6). A short section of SBR rubber hose is mounted to the bottom of the cylinder to simulate Triton's depth tube. Coupons of composite epoxy cylinder sections and SBR rubber hose sections will additionally be installed to study biofouling accumulation of the raw materials.

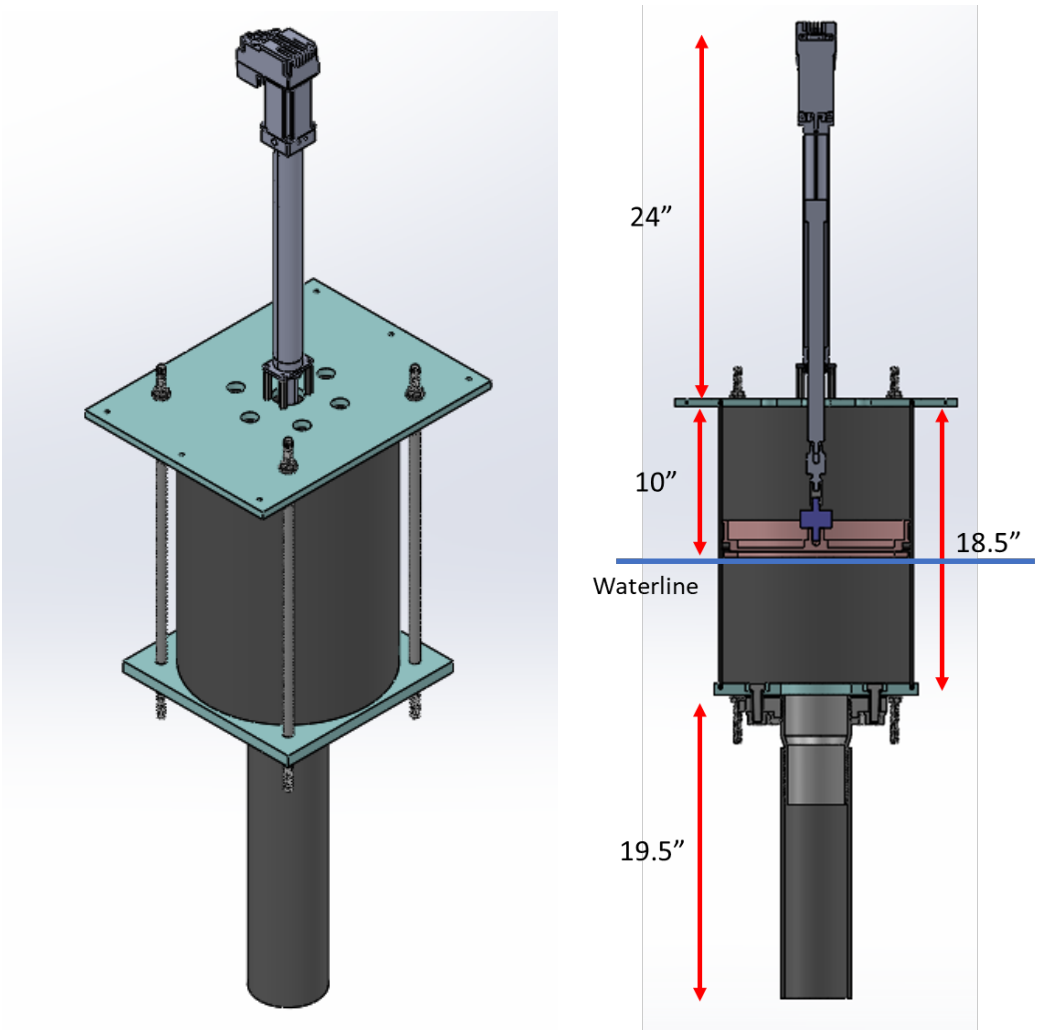

Figure 6: Device Under Test

This test article would be installed in a PNNL Biofouling tank to study the results of biofouling over time. Two identical articles will be installed in the tank. One of the systems will have a biofouling mitigation seal and the other will not, allowing for an evaluation of the seal’s effectiveness

Each test article will have a ball-screw linear actuator that will drive the piston head. This will happen at a predetermined interval to mimic wave action. This linear actuator will have a 10” stroke, supplied with 24 VDC, and driven by a servomotor.

Actuator details:

Tolomatic’s Actuator Sizing tool was used to select an actuator for this application. A 100lb loading scenario was use with an average speed of 0.5in/s. The tool recommended an ERD15 actuator and selections were refined and confirmed by a local representative. The official part number is ERD15 BNM05 SM310.000 LMI ST1 AMI2C1A1 FFG ALC ARI CR58.

Table 1: Actuator Details

Item	Detail	Description
Manufacturer	Tolomatic	
Model	ERD15	Rod-style actuator
Stroke length	310 mm	
Motor	ASCI DC integrated servo	NEMA 23 frame size
Excitation	24 VDC	External power supply
Coupler	ALC	Alignment Coupler
Pitch	BNM05	5mm Ball Screw

Motor Specifications:

A motor specification curve (Figure 8) for torque that shows that the loading requirements are well under the motor's performance limits. The green line is continuous torque while the red line is peak torque. The expected continuous power usage is 10.86 watts.

Figure 7: Tolomatic ERD Actuator

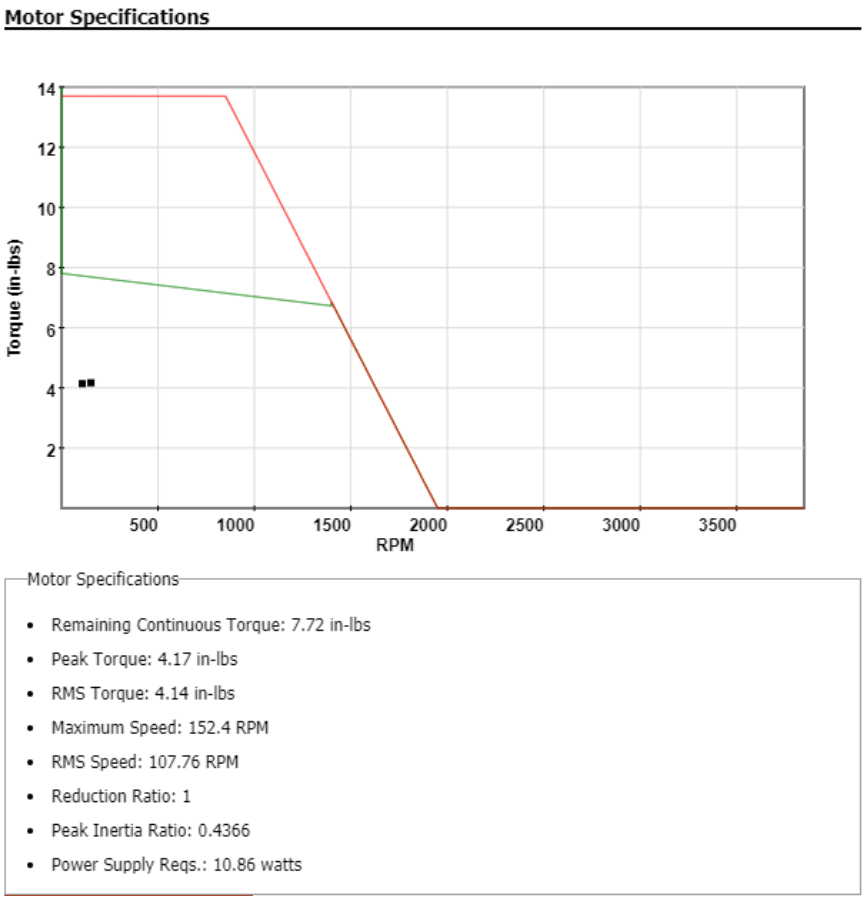

Figure 8: Motor Specifications for Tolomatic ERD Actuator

Power Supplies:

- Mean Well LRS-350-24: AC-DC power supply has a 120VAC input and 24VDC output with a power rating of 350 watts. This powers both actuators.
- Mean Well LRS-35-12: AC-DC power supply has a 120VAC input and 12VDC output with a power rating of 35 watts. This acts as a keep-alive power supply when the main power supply is turned off. The keep-alive allows the driver to remember actuator stroke location and program status.

Cylinder assembly details:

The cylinder will consist of a composite epoxy tube. The cylinder is secured between two aluminum plates with tie rods and sealed by o-rings. Care will be taken to ensure even compression of the o-rings and centering of the cylinder with respect to the piston. The alignment coupler in the piston will allow for some slight misalignment.

Piston Seal Configuration:

The piston seals comprised of three components: biofouling mitigation seal (wiper), wear band, and dynamic seal. This seal configuration is shown in Figure 10. The efficacy of the biofouling mitigation seal will be tested against a control that does not contain this seal.

The biofouling mitigation seals has a wiper configuration and is constructed from a high-performance sealing material for use in hydraulics, oil water emulsions, water hydraulics, and food machinery. This material offers very low wear, as well as exceptional compression set and extrusion resistance.

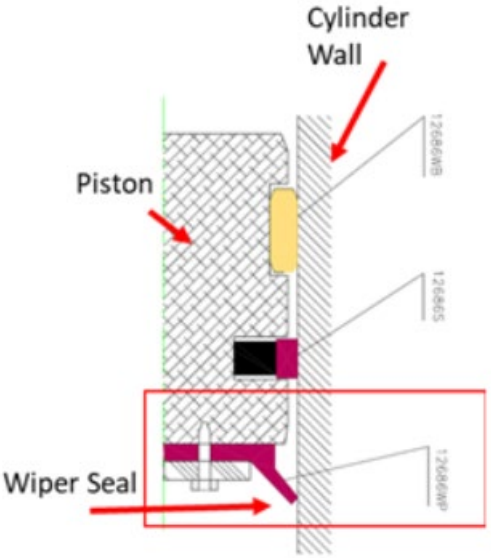

Figure 9: Piston detail depicting seal and wiper arrangement

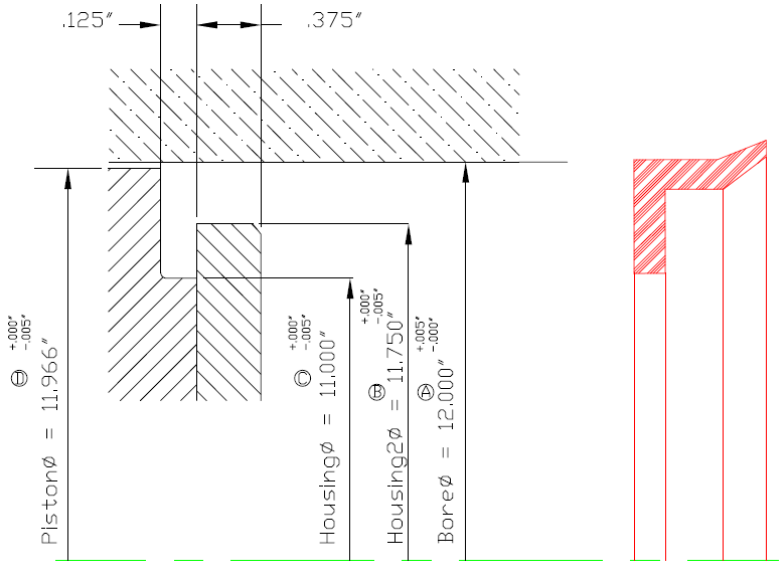

Figure 10: Wiper Seal Drawing - C-12686WP

The wear band, shown in Figure 11, is constructed from a filled PTFE for use as a low-friction guide tape material that offers low friction, low wear and superb chemical properties.

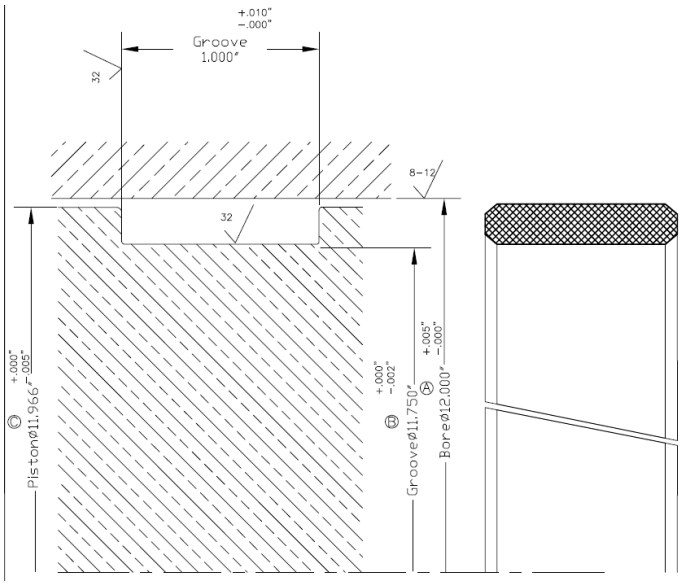

Figure 11: Wear Band Drawing - C-12686WB

The dynamic seal is also constructed from material that offers low wear, as well as good compression set, tear strength and flexibility.

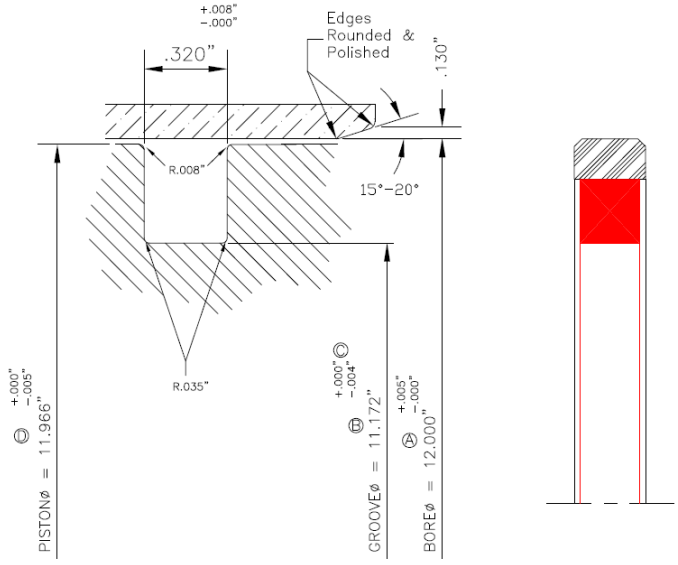

Figure 12: Dynamic Seal Drawing - C-12686S

Stroke limits:

Figure 14 shows the limit of the actuator stroke during test. This leaves space both above and below the stroke limit for evaluation of growth.

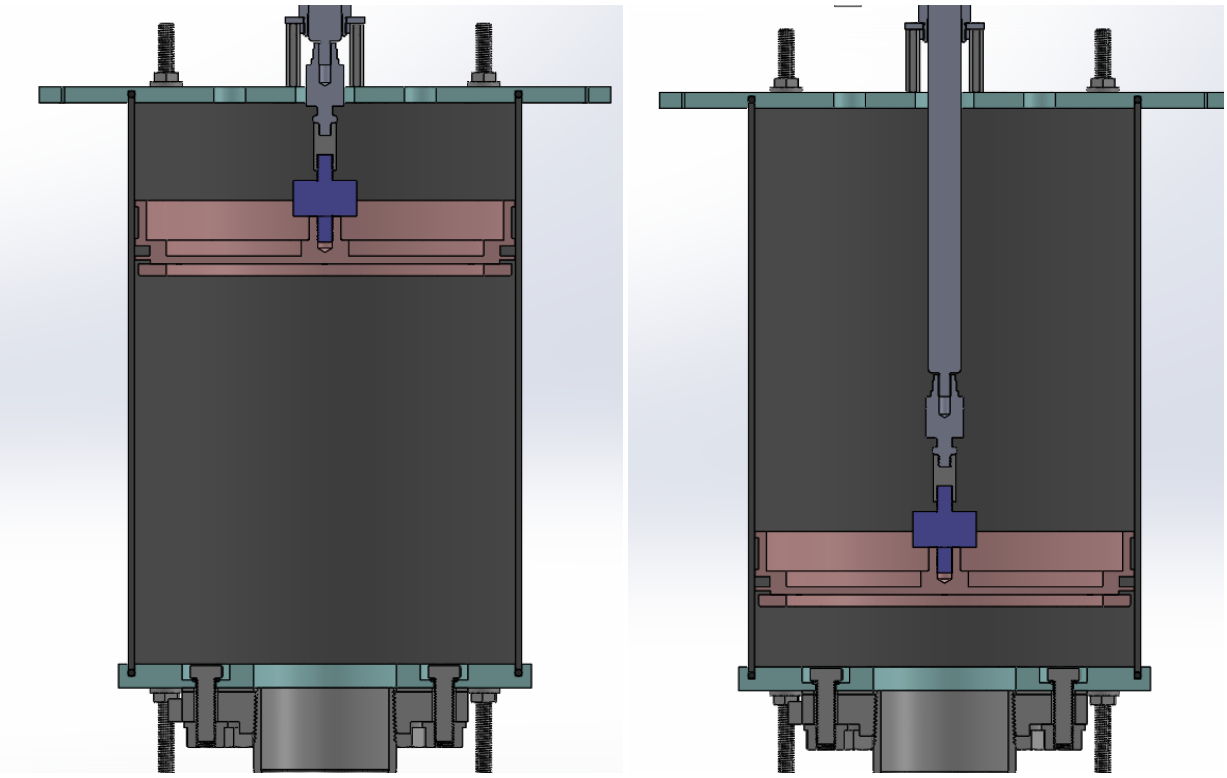

Figure 13: Stroke of actuator during test

Depth tube and bottom flange

The depth tube is constructed from off the shelf McMaster parts. The hose is 16” long and is made from SBR rubber. The hose is secured to a 4 NPT barbed fitting (PN 5363K29) constructed from aluminum. The barbed fitting is threaded into a low-pressure aluminum flange (PN 44705K238). This flange is sealed to the aluminum baseplate with a Buna-N gasket (PN 9165K65). This gasket set contains phenolic washers and PET sleeves that separate the dissimilar metals in the assembly to prevent corrosion. The flange is secured to the baseplate with Sealing hex head screws (PN 92205A533). These screws are made from 18-8 stainless steel and have a silicon rubber o-ring.

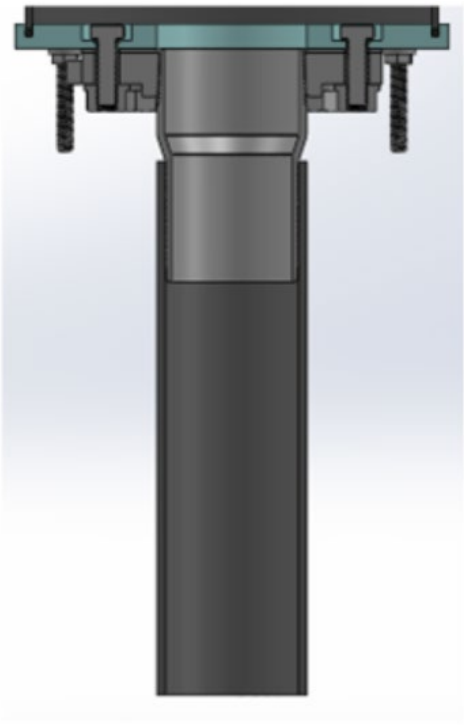

Figure 14: Depth Tube and Flange

Coupon specifications

Two types of coupons will act as static biofouling controls: composite epoxy cylinder and SBR rubber hose. Composite epoxy cylinder coupons will have a 4” inner diameter and will be 4” long.

SBR Rubber hose: This off-the-shelf hose is a stand in for Triton's custom flex-hose design. The McMaster PN is 5289K29. The hose has a 4" inner diameter, 4.5" outer diameter, and will be 4" long.

Mounting features
The upper baseplate of the device under test has holes for mounting to aluminum test frame.

Advancement of marine energy technologies

This test will advance marine energy technologies by evaluating the performance of a biofouling mitigation seal when used in a marine environment. If the seal performs as expected, marine energy devices that use pistons can leverage the seal to prevent or reduce biofouling, increase time between maintenance, and reduce premature failure.

The test of the composite epoxy cylinder will evaluate the use of a composite tube in a marine environment. This material could provide an alternative material for marine energy technologies since it is corrosion resistant, strong, and lightweight.

6 WORK PLAN

6.1 EXPERIMENTAL SETUP, DATA ACQUISITION SYSTEM, AND INSTRUMENTATION

General Work Plan

Work will be conducted to qualitatively describe and quantitatively measure the growth or accumulation of biofouling while measuring the forces acting on the device under tests' pistons, emulating WEC PTO action, over time in an environment conducive to the growth of marine biofouling organisms. Working hypotheses being evaluated through this testing are:

- An emulated PTO unit with a biofouling mitigation seal will develop a *lower mass* of accumulated fouling organisms over time compared to an identical control PTO unit without this seal
- Piston force will initially be *higher* for the biofouling mitigation seal-equipped PTO due to increased friction compared to the control PTO
- Piston force will *become lower* than the control PTO as accumulation of fouling in the control PTO occurs at a *faster rate*
- Wear on the main seal is *lower* with biofouling mitigation seal-PTO due to less fouling on the cylinder
- The biofouling mitigation seal will prevent fouling material from accumulating between the mitigation seal and the first piston seal, or between the piston seals

The experimental apparatuses, methods, and test matrix described below are designed to evaluate these hypotheses.

Biofouling Experimental Procedure and Documentation

The following procedure will be utilized to qualitatively and quantitatively measure the biofouling accumulation of the devices under test.

1. Devices under test will be weighed using a precision scale in their initial dry configuration prior to insertion in the test tank
2. Devices under test will be immersed in filtered seawater and maintained water level for one week
3. The interior of the cylinder will remain dark (except when measurements are taken) to replicate conditions during operation (with a long descending tube)
4. Devices under test will be removed from the tank, imaged, and weighed to establish baseline 'wet' conditions with no biofouling accumulation
5. Testing operation will commence with active force measurement with devices immersed in unfiltered seawater to the same water level and piston stroke and period parameters
6. Piston operation will be paused after each complete 30 day period of operation and devices will be removed from the test tank
7. The interior of the device cylinders will be imaged, their internal diameters (of the tube and accumulating biofilm) measured with calipers, and weights measured on a precision scale
8. Seals will be imaged and inspected for tears, gouges, or other damage.
9. Measurements and qualitative descriptions will be recorded in a laboratory notebook and signed and dated by a laboratory technician or engineer
10. Devices will be replaced in the tank and the procedure from step 4 will be repeated for the 9-month duration of the experiment
11. Control samples (cut sections or squares) of the composite epoxy tubing material will also be prepared, pre-weighed, and exposed to seawater (maintained in darkness) to assess the extent of fouling on this material (independent of the piston operation)

Load Cell Measurements and Data Acquisition

Piston force is measured by the load cell, which outputs a low voltage proportional to the applied load when excited by a constant DC voltage. A load cell amplifier and signal conditioner provides the excitation voltage, and with a preset gain, amplifies the low-voltage signal to a level matching the range of the analog signal data acquisition (DAQ) unit. The gain is selected such that the full rated load corresponds to the highest possible input voltage of DAQ. In this case, a 200 lb force would translate to a 10 V signal into the DAQ after setting the appropriate amplifier gain. Load is linearly proportional to load cell output per the manufacturer-supplied calibration certificate and the acquired voltage through the amplifier. Piston force will be acquired at a rate of 20 Hz for the duration of the experiment. This rate is at least 20X faster than the piston actuation period at full stroke, enabling detailed force feedback throughout individual piston cycles. Identical force measurement systems for the test articles with and without seals will allow for direct comparisons piston force, translating to system efficiency and performance. Components of the force measurement and data acquisition system are found in the table below.

Table 2: Piston Force Measurement Components

Sensor/Item	Range and Rate	Accuracy /Resolution	Calibration	Physical measurement	Output	Purpose /Justification
Omega LC203-200	200 lbf	+/- 15% linearity +/- 0.1% hysteresis +/- 0.05% repeatability	5-Point NIST Traceable Calibration with 59 kOhm Shunt Cal Data	Force [lbf] in tension and compression	2 mV/V of excitation at full load	Piston force measurement, required for process monitoring and seal and mitigation seal performance comparison
Measurement Computing USB-1608G or similar	+/-10 V, 0.0149 Hz – 250 kHz	16-bit analog to digital conversion	N/A	Voltage [VDC]	Digital via USB	Signal acquisition, required for recording force measurements
Omega DMD4059	0-400 mV	N/A	N/A	N/A	+/-10 VDC amplified output, 0-10 VDC excitation	Filters, amplifies, and converts mV load cell output to higher voltage

Load Cell Data Software and Data Processing

The DAQ will be configured utilizing Measurement Computing DAQ software provided by the manufacturer to specify input range, continuous sampling rate, and data storage format. Raw data files will be converted to Matlab .mat format for post-processing in Matlab. Processing scripts will be used to prepare for analyzing the data (detailed below).

Biofouling Material Post Processing and Analysis

Upon completion of the experiment due to the end of the specified testing period or inoperability of the device(s) under test, final images and weights will be recorded. A post-processing procedure will be conducted according to the following steps:

1. Devices under test will be disassembled and the composite epoxy cylinder removed
2. The piston assembly will be analyzed to determine if any gaps exist between the mitigation seal and cylinder wall at rest or during actuation

3. Fouling accumulation inside the cylinders will be measured and compared between the piston assemblies with and without a mitigation seal, specifically including the zone below the piston assembly stroke, where the mitigation seal contacts the cylinder wall, and where the piston seals make contact with the cylinder wall
4. The piston assembly will be disassembled to look for and quantify (wet and dry mass) any accumulation of interstitial fluid and fouling material between the mitigation seal and first piston seal (mitigation seal assembly only), and between the first and second piston seals (both mitigation seal and mitigation seal-free assemblies)
5. Visual inspection will characterize the type (e.g., presence of microbial slime, algae, and hard or soft fouling species) and location of fouling within the devices
6. A biological staining and imaging procedure will be used to quantify fouling on the control samples of composite epoxy tubing and within different sections (below the piston stroke, active mitigation seal zone, piston seal zone) of the devices
7. Wet and dry weights will be determined to further quantify the accumulation of fouling material
8. The mitigation seal and piston seals will be examined for signs of wear and abrasion.

Description of biofouling measurements. Wet weight measurements are made by removing a sample from water and using a blower to remove unincorporated water from the material surface, leaving only the fully hydrated organisms. Dry weight measurements entail baking a sample for 12-18 hours in a 50°C oven to remove water from the sample prior to measuring the weight of the sample. Comparing the wet and dry weights provides and assessment of the contribution of 'soft' organic matter and 'hard' calcium carbonate or silica to the fouling complex. The staining and imaging protocol uses a mixture of biological stains to reveal organic matter and cells on a surface. The quantity of fouling material determines how much stain is accumulated and image processing software calculates the quantity of fouling material present based upon an analysis of color density extracted from digital photographs.

Coupon Material Testing

At biweekly intervals, a coupon from both the composite epoxy cylinder and SBR hose will be removed and analyzed. Images at 30 day intervals should allow for direct comparison of coupons to devices under test.

6.2 Test and Analysis Matrix and Schedule

Project Schedule

Testing as specified in the above sections will occur over a period of 9 months following setup and initialization.

Task/Month	1	2	3	4	5	6	7	8	9	10	11	12
Design and Planning												
Setup												

Active Testing												
Analysis												
Reporting												

Test Parameters/Matrix

The actuator has a 12” stroke; 10” of the stroke will be used for testing. This leaves space at the top and bottom of the cylinder for observation. The center of the stroke will sit at the waterline

The piston will move at an average speed of 1 in/s over the 10” stroke in a pure sinusoidal motion resulting in a full period of 20 s, held consistent throughout testing. The selected period represents the higher end of actuation period to be expected from wave action. Every 12 hours, the piston will rest for 30 minutes.

6.3 SAFETY

All work scopes and funding must be authorized by one or more responsible managers, depending on the type of work being performed, and all work activities conducted in laboratory or operations spaces must be conducted under a project management office director approved electronic prep and risk (EPR) profile and appropriate work planning and controls.

Hazards and risks associated with the work follow the requirements in hazard-specific work controls and are reviewed with assistance from the PNNL Safety and Health representative, and/or PNNL subject matter experts (SMEs).

Standard controls to mitigate hazards are conducted in the following order:

- Elimination or substitution of hazards
- Enaction of engineered controls
- Performance of specified work practices and administrative controls
- Use of personal protective equipment

Determination of appropriate work controls relevant to the work performed are found in a PNNL Lab Assist document. A Lab Assist activity is a central document that includes work controls, applicable training, associated hazards, and approved lab spaces that all workers must review and acknowledge before performing work. All workers performing activities on this task will be required to review hazards, mitigations, and engineering controls listed within the Lab Assist activity and complete trainings as appropriate prior to the onset of lab work.

6.4 Contingency Plans

There are risks associated with the work where issues would result in being unable to complete test objectives, outlined with mitigation/contingency in the table below:

Table 3: Risks and potential mitigation strategies

Risk	Mitigation/Contingency
Seal failure	Spares available for replacement after documentation of failure mode
Fouling accumulates to the point of disrupting functionality of piston	This is an acceptable endpoint of the experiment
No or little measurable fouling accumulation	Request extension of performance period
Unforeseen failure mode of apparatus (e.g., part corrosion causes leak)	Consult with Triton Systems Inc. on a suitable repair or return unit and repeat testing

6.5 Data Management, Processing, and Analysis

6.5.1 Data Management

- Quantitative and qualitative biofouling measurements and descriptions will be recorded in a laboratory notebook and signed and dated by the technician or engineer conducting the assessment. The notebook entries will be digitized into MS Word and Excel documents and stored on MS OneDrive for backup and archival purposes

- Force measurements and associated timestamps recorded by the DAQ will be stored locally on a PNNL computer and uploaded to MS OneDrive in raw .csv and pre-processed .mat files

Table 4: Data to be uploaded to MHKDR

Data	File Type(s)	Description
Piston force measurements	.csv, .mat	Force in lbf and/or N, time for both raw and processed data
Test article weight	.xlsx	Apparatus weight in lbf and/or N, time after initial immersion, notes

6.5.2 Data Processing

Load Cell Data Processing

Raw force data from the load cells will be processed using the following steps:

1. Low-pass filtering the data to remove high-frequency electrical noise, identified utilizing a Fast Fourier Transform on the raw force measurements
2. Conversion to engineering units using load cell calibration and amplifier gain setting
3. Time averaging the filtered data over relevant periods (e.g., days, weeks, months) for bulk comparison of piston load
4. Phase averaging the filtered data for detailed comparison of forces through piston stroke

Uncertainty in load measurements may be calculated by summing the systematic and statistical errors; the former is derived from specifications of the load cell, and the latter is quantified as the standard deviation of the mean of measurements over averaging periods. Data QA/QC will be conducted through statistical functions native to Matlab, replacing spurious data points with NAN values.

6.5.3 Data Analysis

Biofouling Analysis

i. Biological growth data for weight and staining efficacy will be processed in triplicate and allow for statistical analysis for mean and standard deviation of mass and percent cover to test for significance. PNNL staff will complete statistical analyses and help Triton Systems interpret test results.

Load Cell Analysis

Time series, time, and phase-averaged load cell data will be compared between the devices to determine trends in loading in the presence or absence of accumulated fouling and the impact of the biofouling mitigation seal. Trends may be correlated to Imaging and qualitative biofouling analysis taken throughout the experiment on monthly intervals.

7 PROJECT OUTCOMES

7.1 RESULTS: PERFORMANCE DATA

Piston force was measured throughout the experiment at a 10 Hz sampling rate utilizing Omega LC203-200 load cells amplified through Omega DMD4059-DC strain signal conditioners, collected with a Measurement Computing USB-2416-4AO data acquisition board and written to a PC. Water temperature measured in the inlet to Sequim Bay by a Nortek 2D Horizontal Profiler ADCP (thermistor embedded in housing) was collected for reference during parts of months 1 and 2. These data, while helpful for viewing general trends, are not intended for performance analysis as temperature in the experimental tank will differ. Water temperature in the tank was measured for part of month 3 and month 4 using an Omega M8MJSS-18-U-12 thermocouple probe, DRSL-TEMP signal conditioner, and M8C-SIL-J-S-F-5 cable. Measurement Computing DASYLab software was used to control data acquisition. A moving root-mean-square (RMS) filter with a window size of 1000 data points is applied to load cell data to smooth and generate a more easily readable and interpretable product showing trends in force over time

(Figure 15). The assembly with the biofouling mitigation wiper is herein referred to as “Assembly 1”, while the assembly without the wiper is herein referred to as “Assembly 2”.

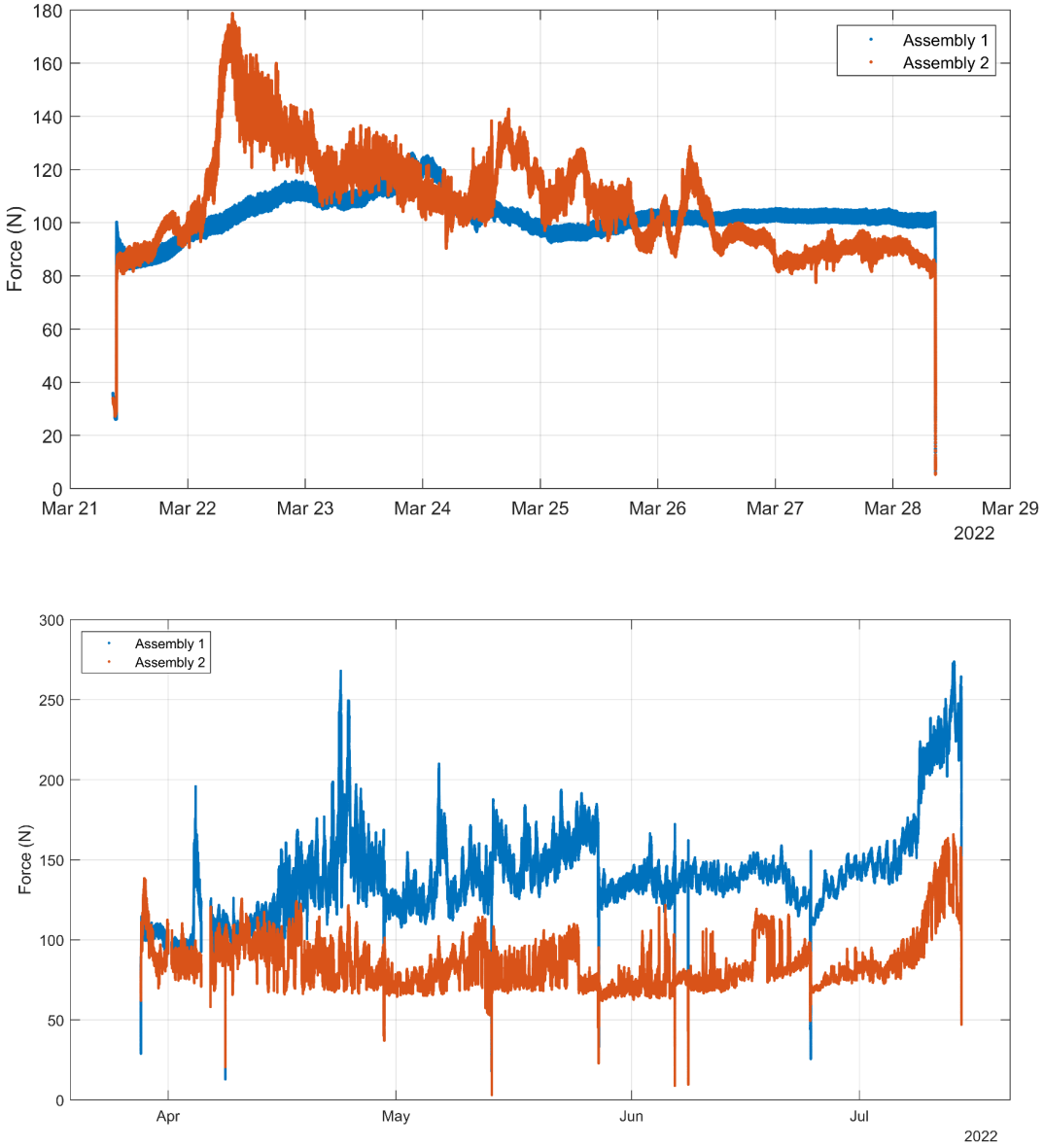

Figure 15: Moving RMS-filtered load cell force with a 100 s filtering window for baseline (top) and core (bottom) testing duration. Low-force spikes are filtering artifacts at startup and shutdown

Baseline/burn-in testing over one week of continuous operation in filtered seawater shows assemblies commenced with similar load profiles before Assembly 1 assumed a more variable and generally higher force trend. Both assemblies reached a similar force level and relatively consistent operation by the end of the baseline period, with Assembly 2 maintaining more consistency.

During core testing, two key trends were shared between assemblies: a strong diurnal cycle of RMS force and lower force after shut-down, removal, inspection, and restart cycles. Diurnal periodicity was

shown to be linked to water temperature during the period in which it was concurrently measured (Figure 16). Assembly 1 experienced higher piston force throughout the majority of the testing period. Summary force data are presented in Table 5.

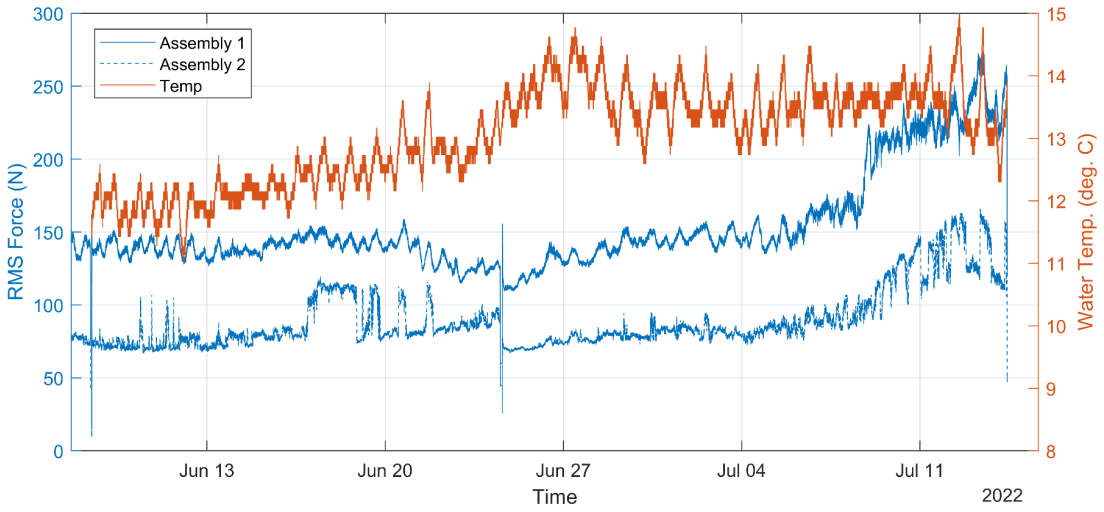

Figure 16: Moving RMS-filtered load cell force with a 100 s filtering window and tank water temperature for partial months 3 and 4 of core testing

Table 5: Summary piston force by testing period

Testing Period	Mean RMS Force, Assembly 1 (N)	Peak Force, Assembly 1 (N)	Mean RMS Force, Assembly 2 (N)	Peak Force, Assembly 2 (N)	Temperature (deg. C) [mean;min;max] Location
Baseline	102.8	254.8	108.2	355.2	
Month 1	125.9	864.7	91.2	353.6	[8.9;8.0;11.2] Sequim Bay*
Month 2	142.3	529.3	80.1	458.2	[9.5;8.7;11.4] Sequim Bay*
Month 3	137.9	400.3	80.1	378.1	[12.3;11.0;13.9] Tank
Month 4	167.3	736.2	95.2	499.1	[13.6;12.3;15.2] Tank

*not intended for performance evaluation

Load cell force was binned based on corresponding temperature readings, and the results are plotted in Figure 17. The general trend demonstrates increasing forces for both assemblies with increasing

temperatures. Boxplots were also created representing force for each temperature bin and assembly, which are included in the appendix.

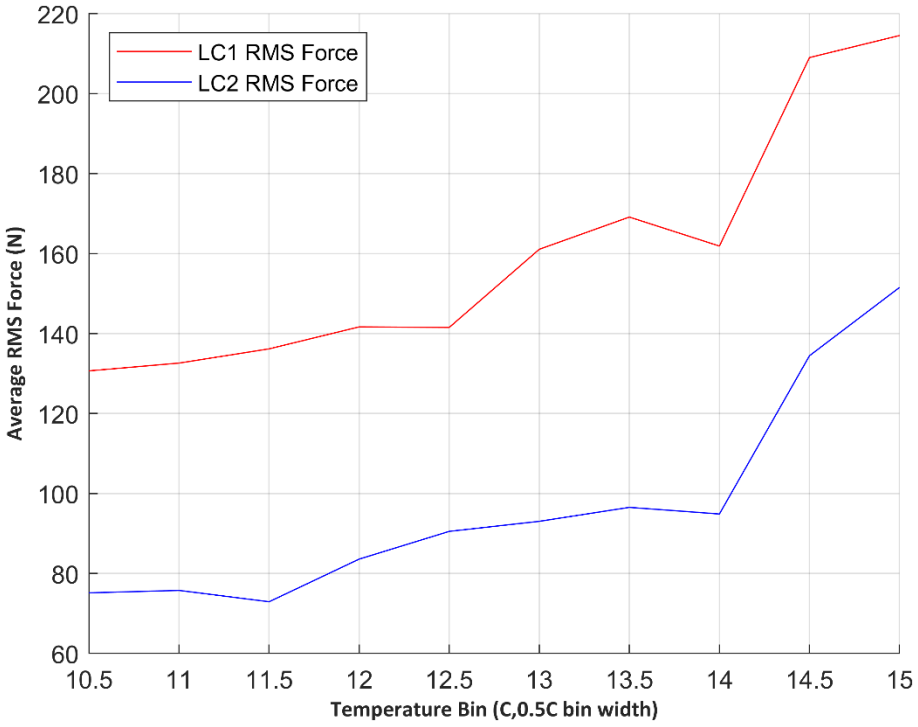

Figure 17: Average RMS force by temperature bin for assembly 1 (LC1) and assembly 2 (LC2)

An additional analysis was conducted to characterize the mean force associated with piston tension and compression across the four months of testing. Raw data were divided into cycles by identifying instances when force transitioned between tension (upstroke) and compression (downstroke) utilizing zero crossings. The average duration of a stroke was calculated to be 10 seconds, so datasets between 5 and 15 seconds in length were selected for analysis. In order to avoid identifying the jitter at beginning and ends of cycles as stroke-transition zero crossings, a mean filter of 2 seconds was applied to raw data. Filtered data were only used to identify cycle transitions; raw force was analyzed during these identified cycles. Next, each stroke's measurements were resampled so they contained an equal number of datapoints regardless of duration. An average stroke was calculated for each month by averaging all cycles within the month for each standardized phase (i.e., datapoint) of the stroke. Results are depicted in Figure 18.

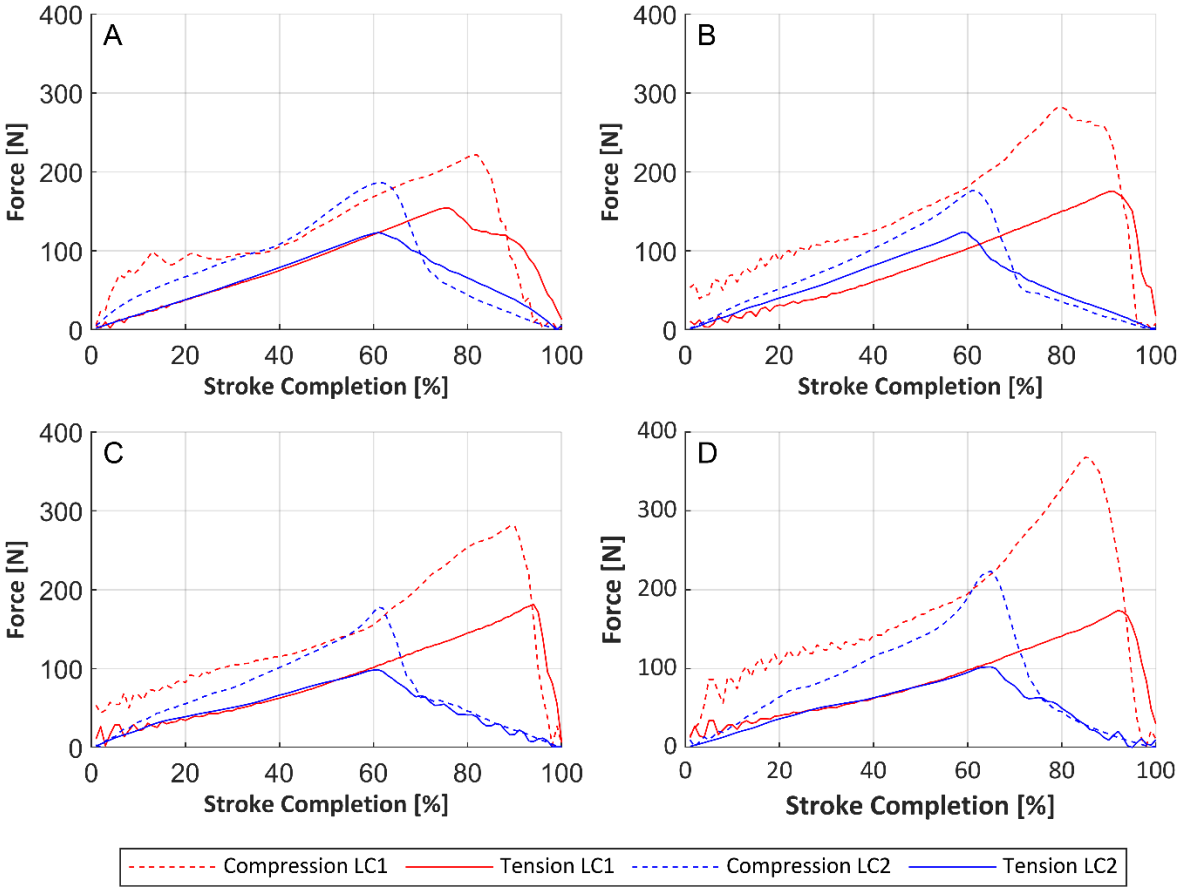

Figure 18: Average tension and compression forces per assembly for months 1, 2, 3, and 4 (A, B, C, and D respectively)

Standard deviation was also calculated for each datapoint in a cycle and is depicted as errorbars representing average standard deviation per 10 datapoints in similar figures for all months, which are included in the appendix.

Some of the jitter at the beginning and end of cycles are evident in the results, particularly in the beginning of assembly 1's strokes. Notably, oscillations increase in the last two months of testing in the falling end of assembly 2's tension strokes. Assembly 2's dynamic seal failed in month 4 leading to the termination of the experiment.

Another notable characteristic in these figures is the difference in location of peak force between the two assemblies. The force seen in assembly 2's strokes drops in magnitude at approximately 60% completion, while assembly 1's stroke peaks closer to 80% or 90% completion. Zero force instances used in separating tension and compression forces correspond to maximum piston velocities, so a peak force 50% through the stroke would likely occur when the piston reached the top or bottom of its swept length. This indicates maximum force in assembly 2 occurred slightly after the piston reversed directions. The offset in assembly 1's peak implies a maximum force much later after a direction change.

Additionally, while assembly 2's compression and tension strokes lasted approximately the same amount of time (median of 10.1 and 9.9 seconds respectively), assembly 1 had greater variation in their length of time (10.6 and 9.3 seconds, respectively). Stroke lengths for each piston are described by boxplots in Figure 19. There was additional variation in the stroke times between months (Figure 20).

The length of time each piston took to complete a full tension-compression cycle decreased from 21 to 17 seconds in months 3 and 4.

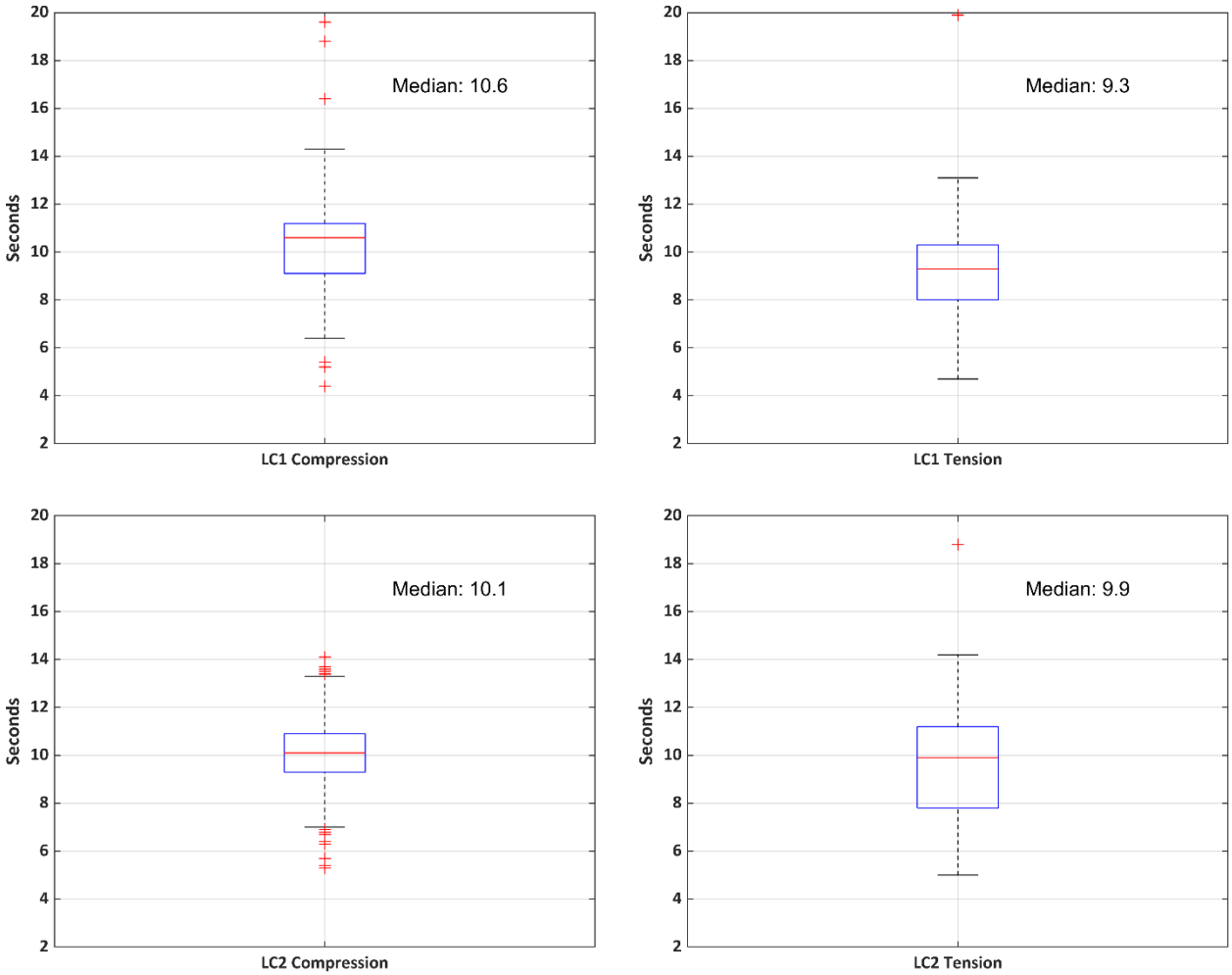

Figure 19: Boxplots of stroke time in seconds for tension and compression per assembly

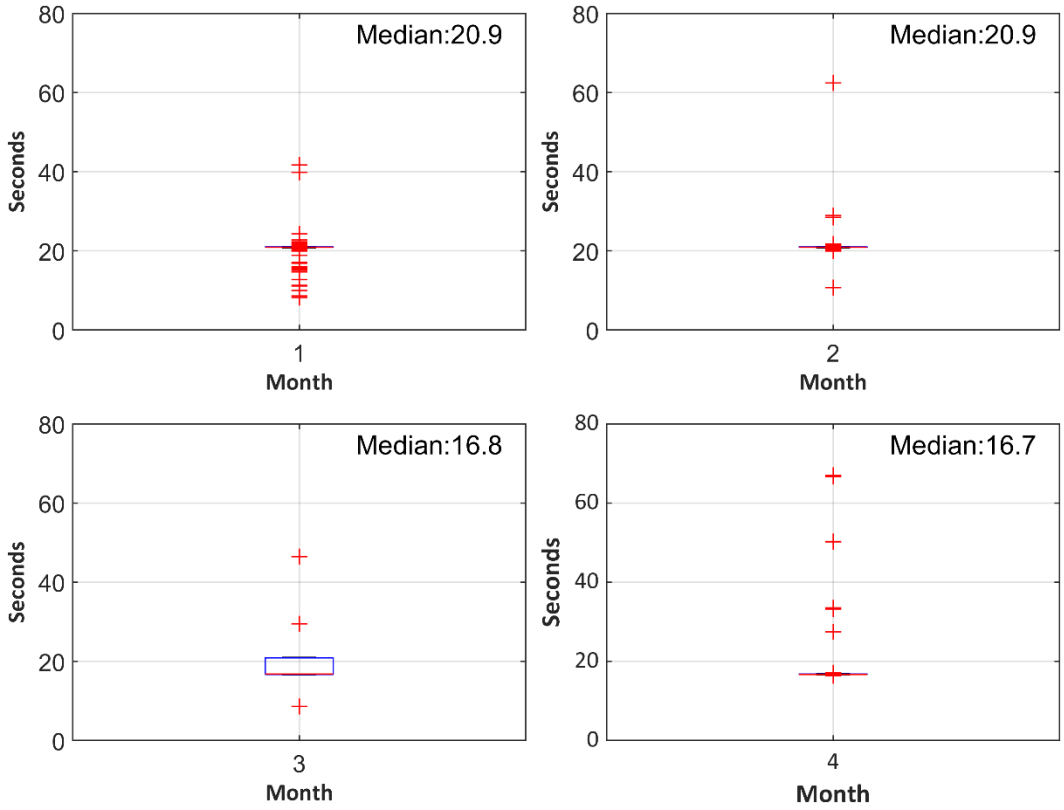

Figure 20: Boxplots of stroke time in seconds of a full tension-compression cycle per month

7.2 Results: Assembly Weights

Biofouling mass was measured throughout the experiment by weighing each assembly while wet after removal from the tank. The assemblies were allowed to drain for approximately one minute before masses were recorded.

Table 6: Recorded monthly assembly weights and net change as calculated from previous month

Date	Mass Assembly 1, Wiper (kg)	Mass Change (kg)	Mass Assembly 2, Control (kg)	Mass Change (kg)
3/28/2022	43.54		43.59	
4/29/2022	43.73	0.19	43.73	0.14
5/27/2022	43.82	0.09	43.82	0.09
6/24/2022	43.50	-0.32	43.77	-0.05

7/15/2022	44.04	0.54	43.95	0.18

The assembly masses reveal an increasing trend with the exception of month 3 (June), where recorded mass decreased for both assemblies. This may be due to one or more of several possibilities: more thorough drainage of water from the assembly before weighing, the disturbance of more biofouling than usual as the assemblies were removed from the tank, or loss of assembly material due to degradation/corrosion or wearing of internal parts.

7.3 Results: Assembly Images

The assemblies were photographed monthly before and after removal from the tanks to document the biofouling growth and corrosion that occurred. Images include the exterior of each assembly, as well as the interior view of the top of each piston and underneath each piston after removing the lower plate.

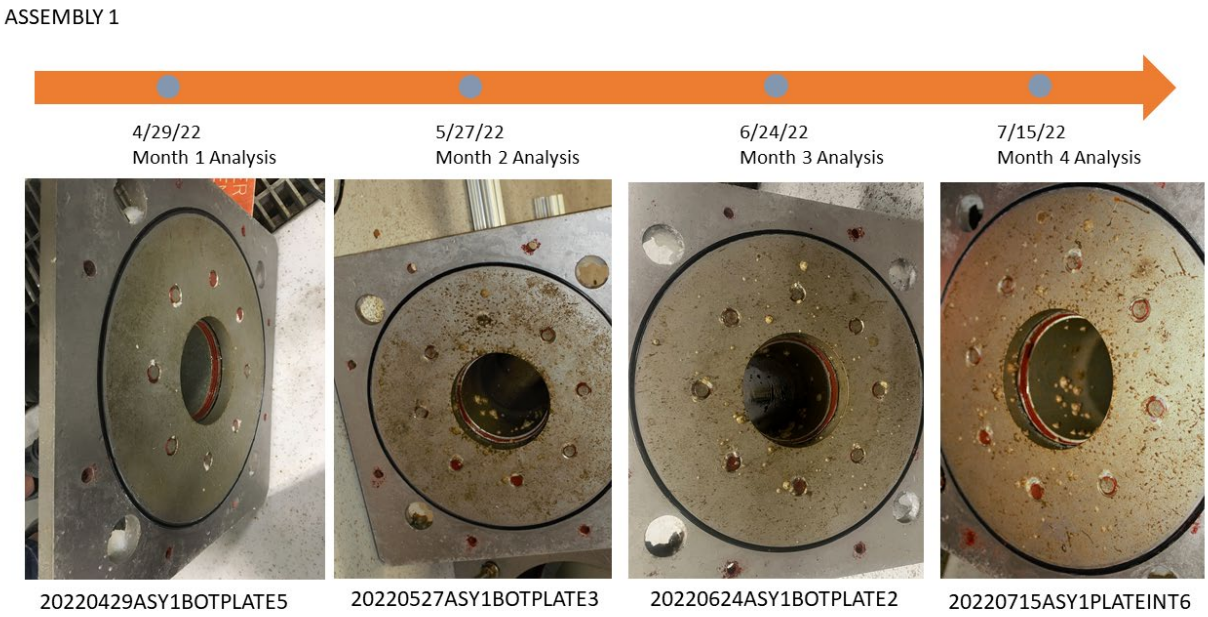

Figure 21: Lower plate of assembly 1 after removal from assembly, photographed at 1 month intervals over 4 months of testing

Photographs of the interior of the lower plate of assembly 1 demonstrate the trend of increasing biofouling over time (Figure 21). Initial findings consisted of a green-brown algal biofilm accumulating on the assemblies, both internally and externally. Small worm-like organisms also appeared on flat surfaces and void spaces (i.e., bolt holes). Small barnacles started growing on the lower plate interior and the inlet tube of both assemblies.

By month 2, barnacles were increasing in size and number, and the white nodules in void spaces appeared larger. A biofilm had begun forming inside the composite epoxy tube below the piston stroke on both assemblies (Figure 23), reaching up into the tube on assembly 2, though to a lesser extent than below the piston's stroke. Both this biofilm and the barnacles continued to increase by month 3, and

additional barnacles were observed growing on the interior of the piston tube but below the stroke of the piston for both assemblies. This qualitative trend was observed to a lesser extent on assembly 1 than assembly 2. At this point a biofilm was also gathering on the top of the piston heads, seen in Figure 22. The biofilm indicated some amount of dynamic seal underperformance, allowing seawater and biofouling to gather on the piston above the seal.

Figure 22: Top of piston 1 before removal of assembly from tank, photographed at 1 month intervals over 4 months of testing

Continuation of the described trends was observed until the assemblies were pulled from the tank for the final time in month 4. Barnacles were more numerous and larger than previously observed, with some measuring as large as 10 mm in diameter. The biofilms interior to the tube and above the piston head continued to grow, as did the white/clear nodules forming in void spaces.

Figure 23: Interior of black tube 2 after removal of lower plate, photographed at 1 month intervals over 4 months of testing

Additionally, black particles (dust/debris) appeared beneath actuators on the head of the load cells beginning in month 1 (Figure 22), and a slight wobble in the actuators was noticed. This was hypothesized to be caused by wearing of bushings or other internal components of the actuators.

7.4 Results: Coupon Samples

10.16 cm diameter coupons of both the SBR hose and piston tube material were immersed in a separate, covered seawater tank to measure biofouling growth on each material in low light conditions, such as in deep water. Coupon masses were measured before immersion in the tank, and at one-month intervals a coupon of each type was removed and weighed. Both wet and dry masses were recorded, where wet masses were taken a few minutes after removal from the tank, and dry masses were taken after leaving the sample in a 60°C drying oven for 24 hours. Wet and dry mass changes over four months are presented in Table 7 below.

Table 7: Material coupon change in mass over 5 months, recorded at 1 month intervals.

Month	SBR Hose Recorded Mass Gain (g)	Composite Tube Material Mass Gain (g)	Wet vs Dry
1	7.8	4.2	Wet
1	0.1	0.2	Dry
2	8.3	2.4	Wet

2	0.4	0.1	Dry
3	8.9	4.3	Wet
3	0	0.1	Dry
4	6.9	6.7	Wet
4	-0.4	0.1	Dry
5	11.1	5.5	Wet
5	-0.3	0.4	Dry

The resulting accumulation indicates that biofouling will present an issue even at depths with minimal sunlight, though measured biofouling accumulation was not linear over time (seen in Figure 24). Most of the biomass accumulation was algal, although sporadic barnacles appeared on various coupons in months 3-5. The larger increase in wet masses compared to dry masses is reasonable considering the algal (i.e., high water content) nature of biofouling and minimal hard growths on the coupons. Months 4 and 5 SBR hose results are of note, as the data indicates loss of mass over this time. It is hypothesized that the material was degrading, which is only noticeable after the removal of water weight through the drying process.

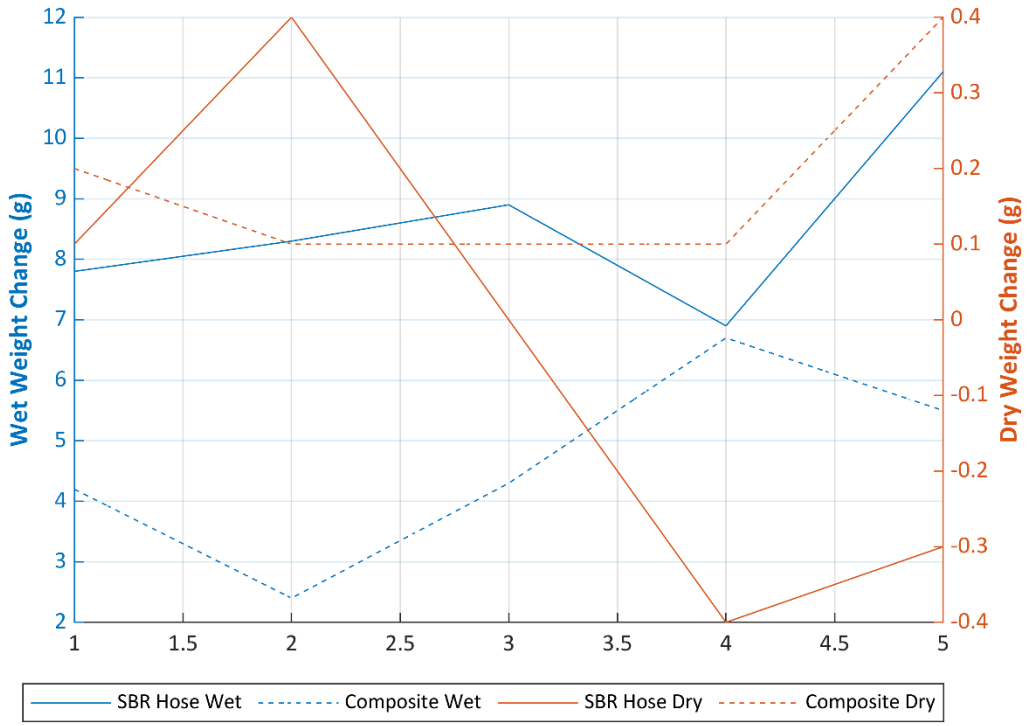

Figure 24: Coupon change in mass over 5 months for SBR hose and composite tube samples, measured both wet and *dry.*

7.5 Results: End of Experiment Biofouling Analysis

Final biofouling buildup on the interior of cylinders and piston surfaces was characterized by weight and by carbon and nitrogen content. Cylinders and pistons were disassembled and rinsed in deionized water, and the resulting mix of water and biofouling was filtered through 0.7 µm then 0.22 µm filters to isolate solid material from liquid for separate analyses (depicted in Figure 25).

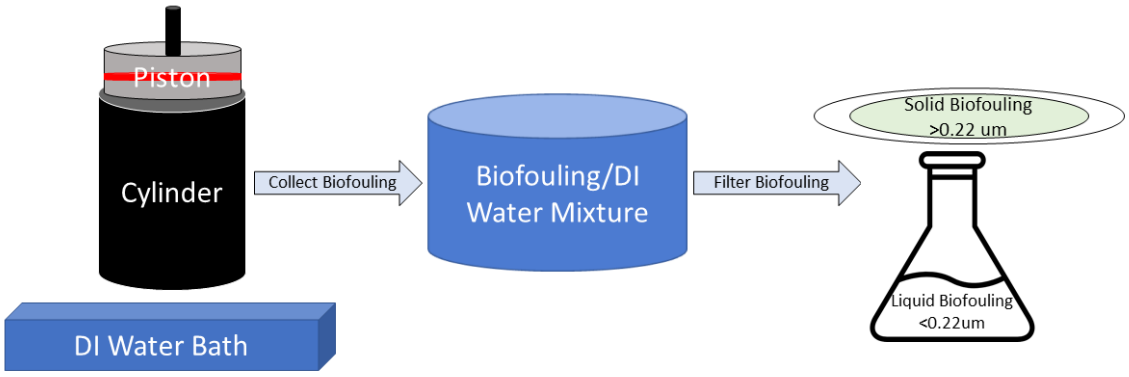

Figure 25: Final biofouling analysis collection process: remove biofouling from piston and cylinder with DI water bath. Collect and filter this mixture to isolate solid material from liquid filtrate.

7.5.1 Solid

Solid samples were weighed immediately after filtration while wet, and total mass was recorded. They were then dried in an oven at 60°C for 72 hours and weighed again to collect total dry mass. Total mass results are presented in Table 8.

Table 8: Total solid biofouling mass collected from each piston and tube, presented for both control and wiper assemblies.

	Wiper Assembly (1)	Control Assembly (2)	Units
Wet Weight	17.4376	12.4191	g
Dry Weight	4.0720	1.4977	g

Assembly 1 (with biofouling mitigation wiper) was found to have more biofouling mass accumulation than assembly 2 (control). It should be noted that most of the biofouling mass was collected from the piston rather than the cylinder, and the majority was found in and above the dynamic seal groove. As water was visible streaking the cylinder sides during the experimental campaign, biofouling above the

dynamic seal is unsurprising. Much of this may be mitigated by an improved dynamic seal, at the cost of higher forces.

After dry weights were measured, samples were subjected to total carbon and total nitrogen (TC/TN) analysis. The solid biofouling was collected from a subset of five filters per assembly and combusted to measure carbon and nitrogen as a percentage of each 5 mg sample using an Orbit Technologies ECS8020 CHNS-O Elemental Analyzer (EA) equipped with an automatic electronic autosampler. Reaction and reduction columns were packed according to operation manual specifications for carbon/nitrogen mode. Furnace temperatures were set to 980℃ for the reactor column, 650℃ for the reduction column and 65℃ for the gas chromatograph. Carrier gas flow was held constant at 110 ml/min and partial pressure set to 1.4 bars. A thermal conductivity detector was used for detection of electrical signals. A calibration curve using an acetanilide standard was created before sample injection to determine the weight percent of total carbon and nitrogen of the gaseous sample, which are reported in Table 9.

Table 9: Total percent carbon and nitrogen in solid biofouling samples from each piston and tube, presented for both control and wiper assemblies.

	Wiper Assembly (1)	Control Assembly (2)	Units
Average Total Carbon	13.716	11.194	% by weight
Average Total Nitrogen	0.492	0.74	% by weight

A standard t-test was performed to determine if the wiper and control average total carbon and nitrogen concentrations are statistically different. Using a two-tailed 99.9% confidence level t-distribution and with calculated carbon and nitrogen t-values of 9.92 and 13.33 respectively, it can be said that the two means came from subsets of different populations. Thus, the control assembly's collected solid biofouling contained a meaningfully higher concentration of nitrogen; however, the wiper assembly's biofouling contained a higher concentration of carbon.

It should be noted that in the solid EA process, carbon is measured as a total combination of organic and inorganic. It does not have the capability to differentiate between the two types. With this limitation, it is possible some of the measured carbon does not originate from biofouling growth. It should also be noted that while the statistical analysis indicates differences in nitrogen and carbon content of biofouling growth between the two assemblies, the sample size of the wiper efficacy test is only one, as one wiper piston was compared to one control piston.

7.5.2 Liquid

The remaining filtrate consisting of DI water and biofouling particles smaller than 22 µm was prepared for dissolved organic carbon and total nitrogen (TN) analyses. Six samples consisting of 9 ml were taken from the water/biofouling mix for each of the control and wiper assemblies, and three deionized water samples were collected for comparison. Dissolved organic carbon was measured as non-purgeable organic carbon (NPOC) converted to carbon dioxide via catalytic combustion. TN was measured by converting nitrogen in the samples to nitrogen gas and detected via chemiluminescence on a Shimadzu

TOC-L Total Organic Carbon Analyzer. Practiced machine operators inspected and confirmed quality of calibration curves and peak shapes prior to exporting data. A summary of the results is presented in Table 10.

Table 10: Average total non-purgeable organic carbon (NPOC) and total nitrogen (TN) content of liquid biofouling and water mixture collected from each piston and tube, presented for both wiper and control assemblies and deionized water.

	Wiper Assembly (1)	Control Assembly (2)	Deionized Water	Units
Average NPOC	8.9535	10.3028	0.3413	mg/L
Average TN	0.94825	0.9844	0.0835	mg/L

A standard t-test was performed to determine if the wiper and control mean NPOC and TN values were statistically different. With calculated t-values of 51.2 and 43.7 and using a two-tailed 99.9% confidence level t-distribution, it can be said that the two averages came from different population subsets. In other words, the assembly with wiper had significantly less average dissolved organic carbon and nitrogen content than the control assembly.

This may indicate an increased biofilm buildup on the assembly without the wiper. The visually inspected biofilm buildup was slow-growing and focused on the area of the cylinder underneath the stroke of the piston. It should again be noted that these results were only available for the single wiper/control set of assemblies undergoing testing, and as such the results of this analysis have an overall sample size of one.

7.6 Lesson Learned and Test Plan Deviation

Test Plan Deviations

Deviations from the original test plan occurred after initial assembly and burn-in testing of the devices under test and after analyzing and reviewing data and results from the first months of core testing.

1. Burn-in operation, intended to allow the assemblies to reach steady-state operating conditions by running in controlled conditions not conducive to marine growth, was planned to occur in static filtered seawater. However, evaporating water hastened salt precipitation onto submerged parts, which was deemed undesirable. The remainder of burn-in testing was completed with filtered seawater continually flowing through the tank, continually replenishing it with natural salinity water.
2. Burn-in testing was monitored and showed increasing piston force over a short period of time, culminating in load cell nominal limitation (890 N) being reached and assembly actuators becoming unable to overcome piston friction. The project team stopped the experiment to disassemble and diagnose the issue. Upon inspection, excessive galvanic corrosion was observed on a sliding bearing element (wear band), creating noticeable accumulation and pitting on the respective dissimilar surfaces. This corrosion is suspected to have drastically increased the friction coefficient of the bearing, leading to excessive force. The part was replaced with a compatible polymeric material alternative and baseline testing resumed within acceptable force range.
3. During core testing, significant force variation on a clear diurnal (24 hour) period was observed, and trending towards increasing variation as the test progressed from winter into spring. The project team decided to integrate a temperature probe directly into the test tank after hypothesizing thermal effects (i.e., material expansion) were responsible for this pattern, corroborated by comparing trends to water temperature measured nearby in Sequim Bay.
4. Performance data were collected at a 10 Hz sampling rate instead of the 20 Hz rate specified in the test plan to reduce file size while maintaining adequate temporal resolution.
5. Material coupons were collected and analyzed monthly instead of bi-weekly, maintaining coupon data collection timepoints equivalent to full assembly analysis timepoints.

8 Conclusions and Recommendations

Testing was highly informative of how the assemblies would perform in open ocean environments. The wiper slightly reduced the formation of biofilm in assembly 1, but hard growths such as barnacles managed to form over time. As the experiment was stopped when the top of assembly 2's piston flooded, the wiper may have been assisting the dynamic seal in assembly 1 in some way, though minor water leakage was present in both assemblies throughout the experiment.

The wiper assembly tended to experience higher mean and peak RMS force throughout the experimental campaign. Though it is likely the extra component accounted for this increased force (through friction), the assembly did not fail due to leaking, as occurred in the control. This information is being used to inform a future iteration of the device under test.

Another key finding of this experimental campaign was the relationship between piston force and cycling temperature of the seawater. As temperatures rose, forces increased, likely due to the different rates of thermal expansion between the piston and the cylinder. This finding is also informing future iterations of the device under test.

Results from this testing directly informed Triton design efforts for future iterations of the wave energy harvesting technology.

Piston Seals

One weakness that was identified very early was an improperly designed sealing set. The original seal design used a dynamic O-ring energized seal and wear band. The energizer specified by the seal manufacturer was too stiff and filled too much of the groove, which would not allow the piston to be installed in the cylinder. A smaller energizing O-ring was specified, but this reduced the seal's effectiveness as there was a slight gap. This seal arrangement was also meant to be self-centering but relied on the original energizer's stiffness. The new configuration caused the piston to cock within the cylinder, increasing friction.

The original wear band material was a bronze-filled PTFE, which quickly corroded. A new wear band was fabricated made from pure PTFE. This wear band performed much better.

Triton used these initial seal findings to improve the piston design for use in a prototype for wave tank testing. This prototype was based on the original TEAMER design. To improve performance, Triton added a second wear band below the dynamic seal on the piston to help center the assembly. This led to better performance during wave tank testing.

In future iterations of Triton's wave energy converter, a pneumatic lip seal replaces the energized dynamic seal. This new seal allows for sealing with a relatively low differential pressure while reducing normal force and overall seal friction.

Piston Material

Another important finding was that small changes in water temperature led to large variations in load cell measurements. It is hypothesized that this is due to differences in the thermal expansion coefficients of the materials in the piston and cylinder assemblies. The piston is made of aluminum, with a high coefficient of thermal expansion. This leads to the piston expanding with warmer water, leading to increased normal force on the seals, resulting in higher friction. In future iterations of the design, Triton will investigate the design of a composite piston that has a low-thermal expansion coefficient to match that of the composite epoxy cylinder.

Composite Epoxy Cylinder

Based on images and biofouling results, the composite epoxy cylinder has potential for use in the marine environment. The smooth inner surface is adequate for dynamic sealing and did not retain significant biomass over the swept portion. As expected, the epoxy material did not react with seawater or experience corrosion. Some wear did occur on portions of the surface, which may have occurred due to cocking of the piston, uneven sealing, or some minor non-circularity.

Dissimilar Metals

This was the Triton team's first iteration of a long-term ocean-going assembly. During this process, and through results from this TEAMER testing, the team became more aware of the necessity of separating dissimilar metals. Galvanic corrosion occurred between some components and necessitated mitigation or replacement.

Triton considers this TEAMER project to be incredibly useful towards the development of a wave energy harvesting system. A large volume of information was collected on performance of the system in a relevant test environment, including performance of the system and materials with respect to biofouling.

Triton will continue testing the prototype with different seal configurations to determine the optimal design. Future in-water testing will monitor temperature of the water and overall friction force to enable full characterization of performance.

9 REFERENCES

10 ACKNOWLEDGEMENTS

PNNL: Kailan Mackereth, Chris Rumple and Alex Barker are thanked for their assistance with setup and teardown of the experiment and multiple iterations of repositioning in and out of the tank.

11 APPENDIX

a. PHASE ANALYSIS PLOTS:

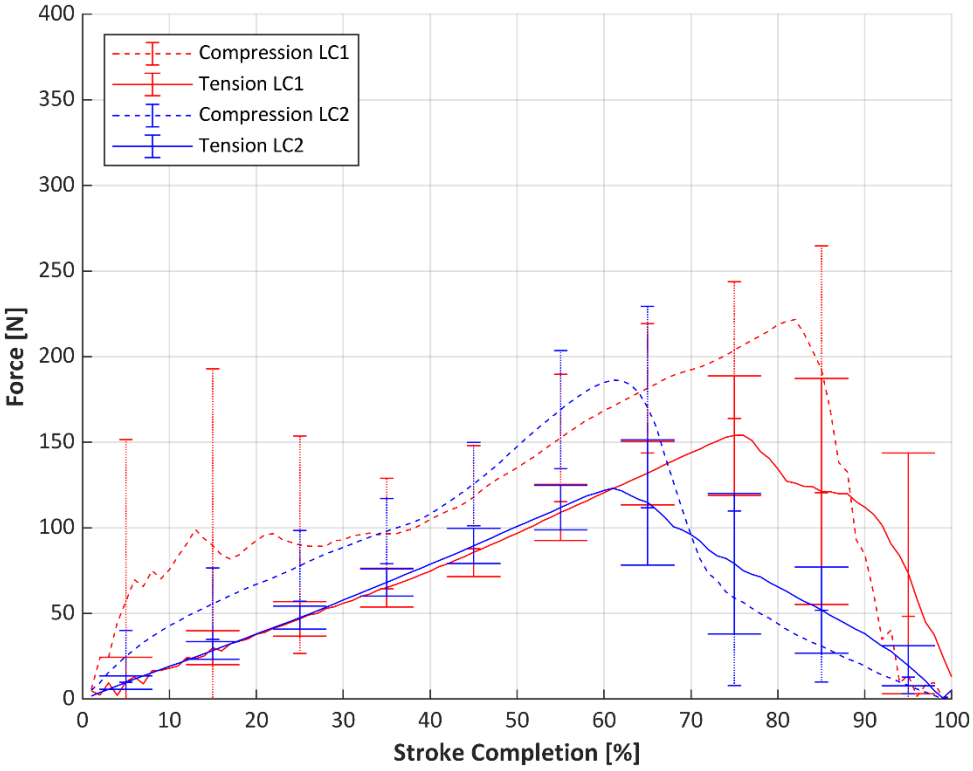

Figure A1: Average absolute load cell force with error bars indicating standard deviation of 10 datapoints for assembly 1 and assembly 2, tension and compression strokes during month 1

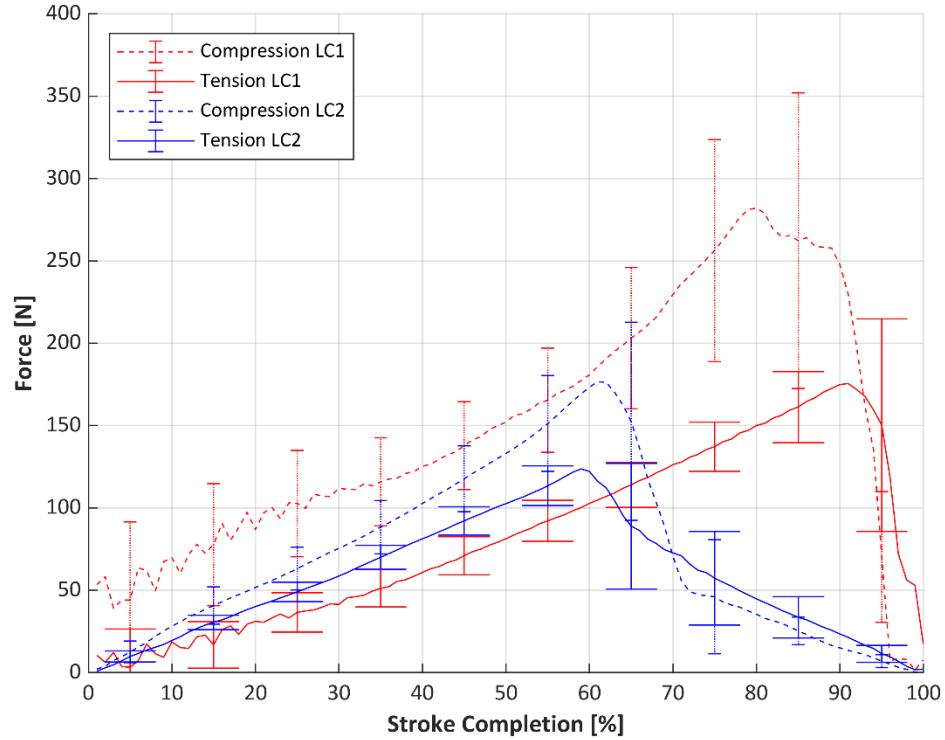

Figure A2: Average absolute load cell force with error bars indicating standard deviation of 10 datapoints for assembly 1 and assembly 2, tension and compression strokes during month 2

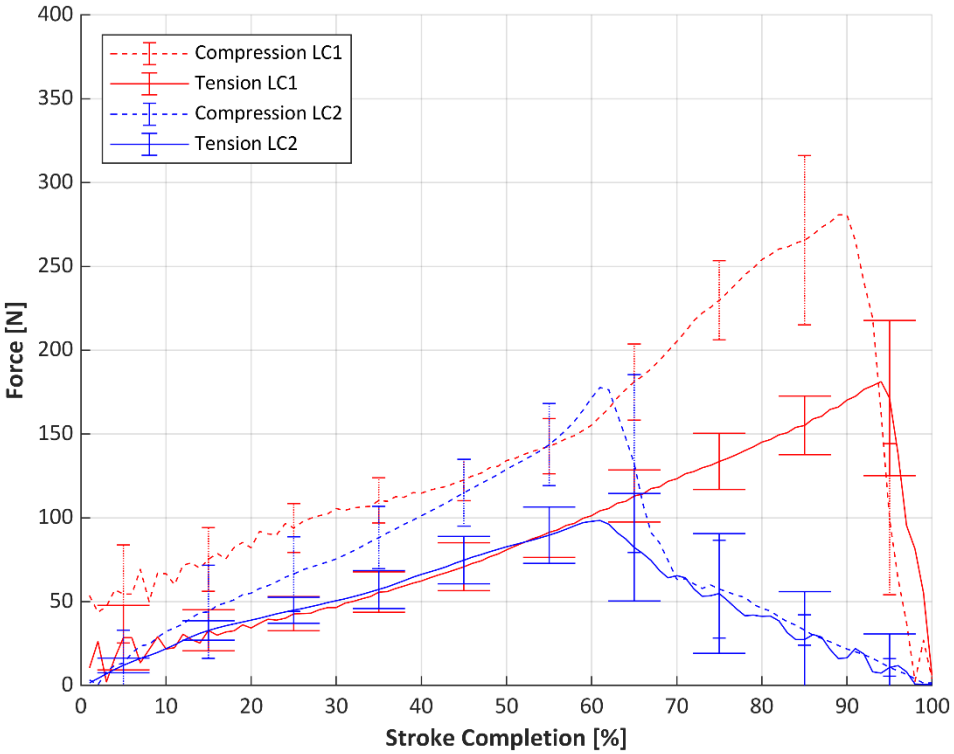

Figure A3: Average absolute load cell force with error bars indicating standard deviation of 10 datapoints for assembly 1 and assembly 2, tension and compression strokes during month 3

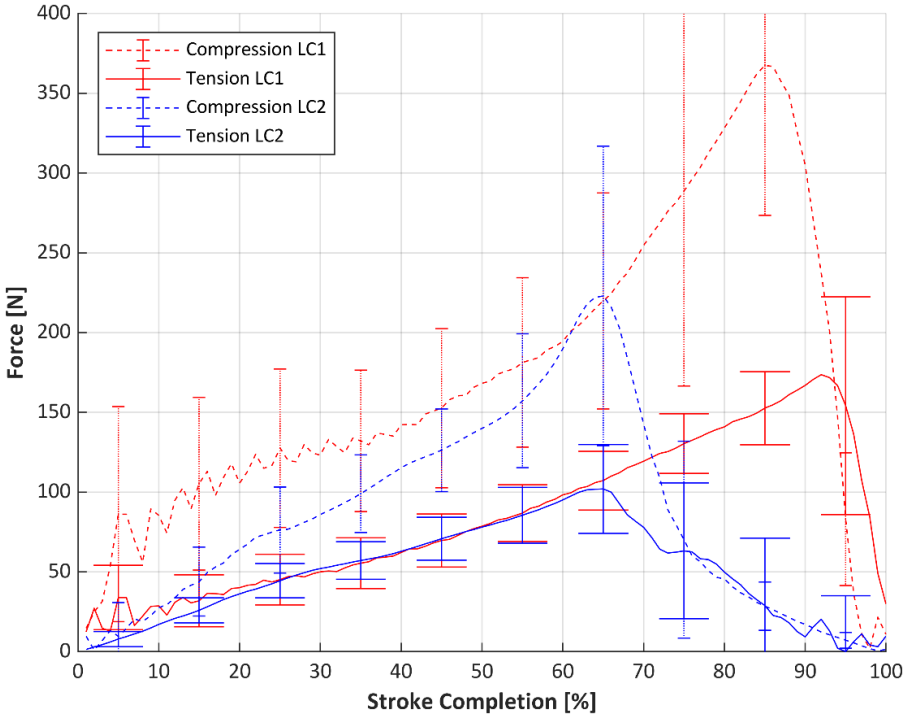

Figure A4: Average absolute load cell force with error bars indicating standard deviation of 10 datapoints for assembly 1 and assembly 2, tension and compression strokes during month 4

b. TEMPERATURE FORCE CORRELATION BOXPLOTS:

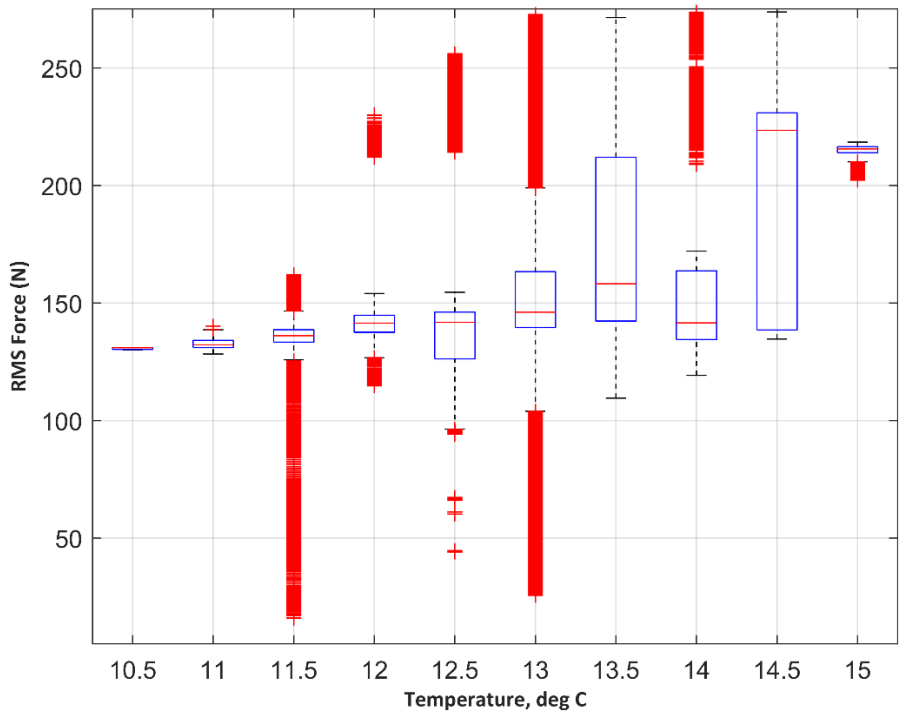

Figure A5: Boxplots describing assembly 1 RMS force by corresponding temperature bin for temperature data collected in the test tank

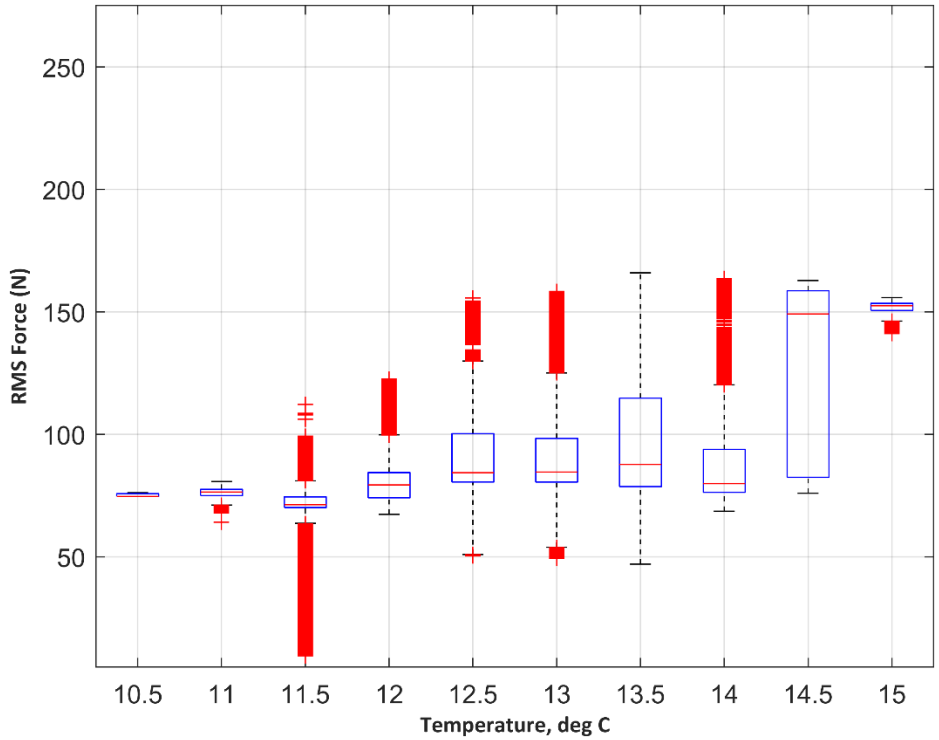

Figure A6: Boxplots describing assembly 2 RMS force by corresponding temperature bin, for temperature data collected in the test tank